Q. J. R. Meteorol. Soc. (1998), **124**, pp. 1831–1860

The ECMWF implementation of three-dimensional variational assimilation (3D-Var). III: Experimental results

By ERIK ANDERSSON[1],* JAN HASELER[1], PER UNDÉN[1], PHILIPPE COURTIER[1], GRAEME KELLY[1], DRASKO VASILJEVIĆ[1], CEDO BRANKOVIĆ[1], CARLA CARDINALI[2], CATHERINE GAFFARD[1], ANTHONY HOLLINGSWORTH[1], CHRISTIAN JAKOB[1], PETER JANSSEN[1], ERNST KLINKER[1], ANDREAS LANZINGER[1], MARTIN MILLER[1], FLORENCE RABIER[1], ADRIAN SIMMONS[1], BERNARD STRAUSS[1], JEAN-NOËL THÉPAUT[3] and PEDRO VITERBO[1]

[1]*European Centre for Medium-Range Weather Forecasts, UK*
[2]*National Research Council, Italy*
[3]*Centre National de Recherches Météorologiques, France*

(Received 20 December 1996; revised 27 August 1997)

SUMMARY

In this third and final paper of a series, we assess the performance of the three-dimensional variational data assimilation scheme, in the light of the results from the extensive pre-operational programme of numerical experimentation. Its performance is compared with that of the previous operational scheme at the European Centre for Medium-Range Weather Forecasts, which was based on Optimal Interpolation. The main features of the new scheme are illustrated, in particular the effects of non-separable structure functions and the improved data usage. TIROS-N Operational Vertical Sounder cloud-cleared radiances, for example, are used directly without a separate retrieval step. Scatterometer data are assimilated in the form of ambiguous winds with the ambiguity removal taking place within the analysis itself. Problems encountered during the tests are discussed and the solutions implemented are explained.

The overall impact on forecast accuracy in the troposphere of the northern hemisphere extratropics is neutral for geopotential and positive for wind and temperature. The impact is neutral in the tropics, and significantly positive in the southern hemisphere. Analyses and forecasts for the stratosphere have improved in all regions. Other positive results include a clear improvement in analyses of near-surface winds over oceans, particularly in the vicinity of tropical storms. This is predominantly because of the assimilation of scatterometer wind-data.

KEYWORDS: Data assimilation Numerical weather prediction Objective analysis

1. INTRODUCTION

A new analysis scheme, based on variational methods (Lorenc 1986; Courtier and Talagrand 1987; Talagrand and Courtier 1987), became operational at the European Centre for Medium-Range Weather Forecasts (ECMWF) on 30 January 1996. It replaced the Optimal Interpolation (OI) scheme (Lorenc 1981; Shaw *et al.* 1987; Undén 1989), which had been operational since the beginning of operational forecasting at ECMWF in 1979. This paper is the third and final part of a detailed description of the new scheme and its characteristics. The companion papers by Courtier *et al.* (1998) (Part I) and Rabier *et al.* (1998) (Part II) discuss the formulation and the structure functions respectively, while this paper (Part III) presents experimental results.

Three-dimensional variational assimilation of data (3D-Var) produces upper-air analyses of temperature, vorticity, divergence, specific humidity and surface pressure for numerical weather prediction (NWP). The analysis is performed directly in terms of the forecast model's spectral representation, on model levels. Analyses are produced every six hours using data from a six-hour time window centred around the analysis time. Observation processing, quality control, background-error computation and surface analysis remain from the OI system in the version of 3D-Var discussed here, although they have recently been replaced by new modules or algorithms.

The purpose of the present paper is to document some of the most important results obtained from a very extensive programme of experiments comparing 3D-Var and OI. We shall try to answer two questions: Have the anticipated improvements materialized? What

* Corresponding author: European Centre for Medium-Range Weather Forecasts, Shinfield Park, Reading, Berkshire RG2 9AX, UK.

were the main difficulties during the pre-operational tests? Some problems emerged and their solutions will be presented here. The degree of balance in the tropical mass–wind analysis was one of the areas which received attention, as did the humidity analysis.

Section 2 gives a general summary of the main features of the 3D-Var analysis scheme, some of which have been presented in greater detail in Parts I and II. The experimental programme is detailed in section 3, followed by a presentation of the overall impact on forecasts in section 4. Section 5 presents results illustrating the main characteristics of the 3D-Var analysis, mainly with respect to the non-separable representation of background errors. The problems encountered during the pre-operational tests, and their solutions are described in section 6. Conclusions and current developments are given in section 7.

2. 3D-VAR FEATURES

Some remarks on 3D-Var's main features are given here in order to guide the interpretation of the results later in this paper. More detailed descriptions have been given in Parts I and II.

(*a*) *Observations*

An important incentive to the development of 3D-Var was that variational schemes are more flexible than OI in their use of observations. 3D-Var allows the relationships between observed quantities and the analysis variables to be *nonlinear*. These relationships (defined as *observation operators* in Part I) can also depend on more than one of the analysis variables. Such observations will have an influence on the analysis of several variables simultaneously, i.e. the 3D-Var scheme is *multivariate* with respect to the observations. Later in the paper we shall examine the influence of radiosonde geopotential data on the humidity analysis, as an example of multivariate effects. The nonlinear and multivariate aspects of the scheme have been studied by Cardinali *et al.* (1994) with respect to two-metre temperature and ten-metre wind data from SYNOP and SHIP reports. The nonlinear and multivariate aspects have also been important considerations in determining the best strategy for the assimilation of satellite data, such as TIROS-N Operational Vertical Sounder (TOVS) radiances and scatterometer winds.

The new scheme is more easily adapted to new types of data. In addition to the data previously used by OI, the first operational implementation of 3D-Var uses TOVS radiance data (Andersson *et al.* 1994) and ambiguous scatterometer wind-data (Gaffard *et al.* 1998). Experiments using total column water-vapour from the Special Sensor Microwave /Imager (SSM/I) instrument of the Defense Meteorological Satellite Programme (DMSP) satellite, are under way (Phalippou 1996; Phalippou and Gérard 1996).

The TOVS data are used directly as radiances after cloud clearing by NOAA/NESDIS (McMillin and Dean 1982; Reale *et al.*. 1986), whereas in OI they are used in the form of layer thicknesses and precipitable-water-content data, retrieved by a one-dimensional variational analysis scheme (Eyre *et al.* 1993; McNally and Vesperini 1996) before the analysis. The use of thicknesses has been retained in 3D-Var in the extratropical stratosphere above 100 hPa and in the Arctic, as will be discussed in subsection 6(c). The incorporation of the retrieval process with the analysis itself, as in 3D-Var, can produce a better combination of the information in the different types of data and in the background (Andersson *et al.*. 1994). TOVS data have a dominant role for the assimilation in the southern hemisphere (Andersson *et al.*. 1991), and later in the present paper we present results showing a clear 3D-Var improvement in the performance of forecasts for that hemisphere.

The scatterometer data are presented to 3D-Var as pairs of wind observations—the two winds in each pair having approximately opposite wind-directions. The choice of

the most likely direction (the so-called ambiguity-removal process) is made during the 3D-Var minimization—a method suggested by Stoffelen and Anderson (1997), using the information in the background and surrounding observations. The use of Earth Resources Satellite (ERS) scatterometer data in 3D-Var has improved the analysis of the low-level wind fields over sea (Gaffard *et al.*. 1998). A tropical cyclone case is presented in subsection 5(e).

(*b*) *Background*

The 3D-Var specifications of observation errors (detailed in appendix B of Part I) and background errors (Part II, subsection 3(a)) are generally more realistic than the OI specifications. The non-separable representation of background errors in 3D-Var is more accurate, especially for temperature, than the separable one used by OI. It gives, for temperature, significantly sharper horizontal correlations and broader vertical correlations. This effect was first discussed by Phillips (1986) and has been discussed thoroughly in Part II. On the other hand, OI has different correlation-structures in different geographical areas which 3D-Var (being global) has not. In other words, the 3D-Var correlation model is non-separable, isotropic and globally homogeneous, and the OI correlation model is separable, isotropic and only locally homogeneous within 'analysis boxes'. There are therefore visible and significant differences between analysis increments produced by 3D-Var and OI, as will be illustrated in section 5. Wind increments are smaller as a result of tuning of background errors and broader vertical correlations; temperature increments are smaller, particularly near the surface, and they have a larger vertical scale in the free atmosphere (giving a very different response to AIREP temperature-data, for example). The stratospheric increments are more large-scale and much smoother in 3D-Var for all variables, because of the increase in length-scale with decreasing pressure given by the non-separable background errors.

Another advantage of the new scheme is that the level of noise (gravity waves) is controlled within the analysis itself. 3D-Var thereby combines several tasks which traditionally have been performed in four separate steps, viz. retrieval of TOVS data, ambiguity removal for scatterometer-wind data, analysis and initialization. This should lead to a better combination of the information in the different types of data and in the background.

3. Experimental programme

The variational analysis scheme has undergone a very comprehensive programme of testing and assessment of its impact, during a period of two years, first at T106 resolution and later at full operational T213 resolution. 3D-Var has been run in parallel with OI at T106 resolution for a total of 146 days in seven separate periods, in all four seasons, and at T213 for a total of 163 days in four separate periods (Table 1). Approximately halfway through the experimentation there was a major change in the forecast model. The prognostic cloud scheme of Tiedtke (1993) was introduced, along with a modified scheme for gravity-wave drag (Lott and Miller 1997) and a grid-point representation of specific humidity together with a revision of the semi-Lagrangian scheme (Ritchie *et al.*. 1995). The initial conditions for the new prognostic cloud-variables are provided by the unmodified first-guess values (Jakob 1994). This new model version is referred to as cy13r4 in Table 1.

All data-assimilation experiments were run with a six-hour cycle, using all data from a six-hour 'window' centred at the analysis time. 3D-Var assimilations were compared with equivalent OI assimilations at the same resolution, using the same version of the model. Ten-day forecasts were run from 12 UTC each day. The forecasts were verified against their own analyses when available, i.e. forecasts from 3D-Var assimilations were verified

TABLE 1. LIST OF DATA-ASSIMILATION EXPERIMENTS IN WHICH 3D-VAR HAS BEEN RUN IN PARALLEL WITH OI

Name	Dates (from–to)	Resolution	Model version	No. of days
A1	1 January 1994–15 January 1994	T106	cy11r7	15
A2	3 March 1994–17 March 1994	T106	cy11r7	14
A3	1 April 1994–15 April 1994	T106	cy11r7	15
A4a	1 August 1993–15 August 1993	T106	cy12r1	15
A4b	16 August 1993–30 August 1993	T106	cy12r1	15
A5	1 October 1993–15 October 1993	T106	cy12r1	15
A6	6 December 1994–17 January 1995	**T213**	cy12r1	**43**
B1	13 June 1994–11 July 1994	T106	cy13r4	29
B2	6 December 1994–2 January 1995	T106	cy13r4	28
B3a	5 April 1995–21 April 1995	**T213**	cy13r4	**17**
B3b	22 April 1995–14 May 1995	**T213**	cy13r4	**23**
B4	24 August 1995–28 October 1995	**T213**	cy13r4	**66**
B5	16 January 1996–29 January 1996	**T213**	cy14r2	**14**
Total				146+**163**

Cycle 13r4 marks an important model change including the introduction of the prognostic cloud scheme. Ten-day forecasts have been run from each day at 12 UTC. Experiments at operational resolution T213 are shown in bold type.

against 3D-Var analyses (otherwise operational analyses were used), and similarly for OI forecasts. Anomaly correlation and root-mean-square (r.m.s.) of forecast error were studied. Forecasts were also verified against radiosonde observations. Two sets of observations not used by either analysis scheme were used to verify aspects of the analyses, namely SSM/I total precipitable water (TPW) for the humidity analysis and ERS-1 altimeter winds for the low-level wind analysis over the sea. Satellite cloud-images were also used in some instances.

The first set of experiments (A1 to A6 in Table 1) produced acceptable results in mid-latitudes, but a deficiency affecting the tropical mass–wind balance was identified. In the continued experimentation, and up to and including the operational implementation, the mid-latitude formulation was kept virtually unchanged as work concentrated on the tropics: experiments B1 to B3 had a multivariate (balanced) tropical analysis; B4 and B5 a univariate one (see Part I). There were some important changes to the humidity analysis in experiment B5, which will be discussed below. The use made of TOVS data was slightly adjusted between each of the T213 experiments. A model change of the shallow convection parametrization was incorporated in the 3D-Var experiment B5, to reduce a systematic overestimation of the height of the trade-wind inversion. It had an impact on 850 hPa temperature-forecast scores and is assumed not to affect the results presented in this paper significantly.

Apart from the assimilations listed in Table 1, many experiments were carried out to test the 3D-Var sensitivity to various types of data (TOVS, ERS-1 and AIREP temperatures), and to some parameters of the formulation.

4. IMPACT ON THE FORECAST

The quality of an analysis scheme for the purpose of NWP is primarily judged by its ability to produce good quality forecasts. In the case of ECMWF, the emphasis is on the three- to seven-day range.

The assessment of the impact of 3D-Var on the forecast turned out to be more difficult than expected. There were very large variations between different two-week test periods (A1 to A5 in Table 1), in terms of 500 hPa mid-latitude forecast scores. 3D-Var was sometimes superior to OI and sometimes the situation was the reverse. There could be periods of five or more consecutive days of very significant difference in forecast performance between the two schemes. Careful study of such periods led to the conviction that very large samples were required to make an accurate assessment. The differences in forecast performance in individual periods could not be ascribed to deficiencies in the 3D-Var formulation or the way data were used. It was concluded that more than fifty cases were required for reliable results. The results of T106-experiments A1 to A6 (not shown) can be summarized as ambiguous for the northern hemisphere, in terms of 500 hPa geopotential, with an indication of a positive result for the southern hemisphere.

(*a*) *Aggregate of large sample*

Given the need for a large sample we shall not attempt to make a distinction between seasons. Instead, we present an aggregate comprising all experiments obtained after the version of the forecast model was changed: experiments B3 to B5 (Table 1). This is the most homogeneous set of experiments available for assessing extratropical performance, with a total of 120 cases. The tropical analysis was, however, modified substantially in B4 which limits us to using B4 and B5 for assessment of the performance in the tropics.

The r.m.s. error in the 500 hPa geopotential, averaged over the 120 cases, is shown for Europe (35°–75°N, 12.5°W–35°E), North America (25°–60°N, 120°–75°W), the northern and southern hemispheres (poleward of 20°), in Fig. 1(a) (b), (c) and (d) respectively. OI is shown as a full line and 3D-Var a dashed line. The panels on the left show the results in absolute terms and the panels on the right in terms of relative differences, expressed as percentages. The vertical bars represent 95% confidence levels in a t-test, (where independence has been achieved crudely by retaining only one value out of three for hemispheric scores and one out of two for European and North American scores before performing the test). We can see a slight advantage for 3D-Var in the European area for days six to eight (Fig. 1(a)). There is a neutral result for North America (Fig. 1(b)) as well as for the northern hemisphere (Fig. 1(c)) as a whole. The result for the southern hemisphere (Fig. 1(d)) is significantly in favour of 3D-Var, from day 2 to day 6.

There is a clear indication that the very short-range (day one and two) scores in the northern hemisphere are slightly worse with 3D-Var. Investigations have shown that this can be attributed to a relatively large-scale forecast-error component, predominantly in the subtropical areas, which clearly does not project on the rapidly growing modes and does not impair the usefulness of the 3D-Var forecasts. The problem may result from an imperfect treatment of tides, or an incorrect specification of structure functions for the largest scales.

Forecast verifications of geopotential at 1000 hPa (not shown) are very similar to those presented for 500 hPa. Verifications of wind and temperature generally show a more positive impact of 3D-Var, than those of geopotential. Wind forecasts at 200 hPa, for example, are clearly better than OI in both hemispheres (Fig. 2(a) and (b)). Figure 2(c) and (d) shows a similar positive result for temperature at 200 hPa.

(*b*) *The stratosphere*

The performance of 3D-Var in forecasts of the state of the stratosphere has been a subject of particular attention in view of the improved description of background errors there (Part II). The verification indeed shows a very substantial gain over OI in terms of

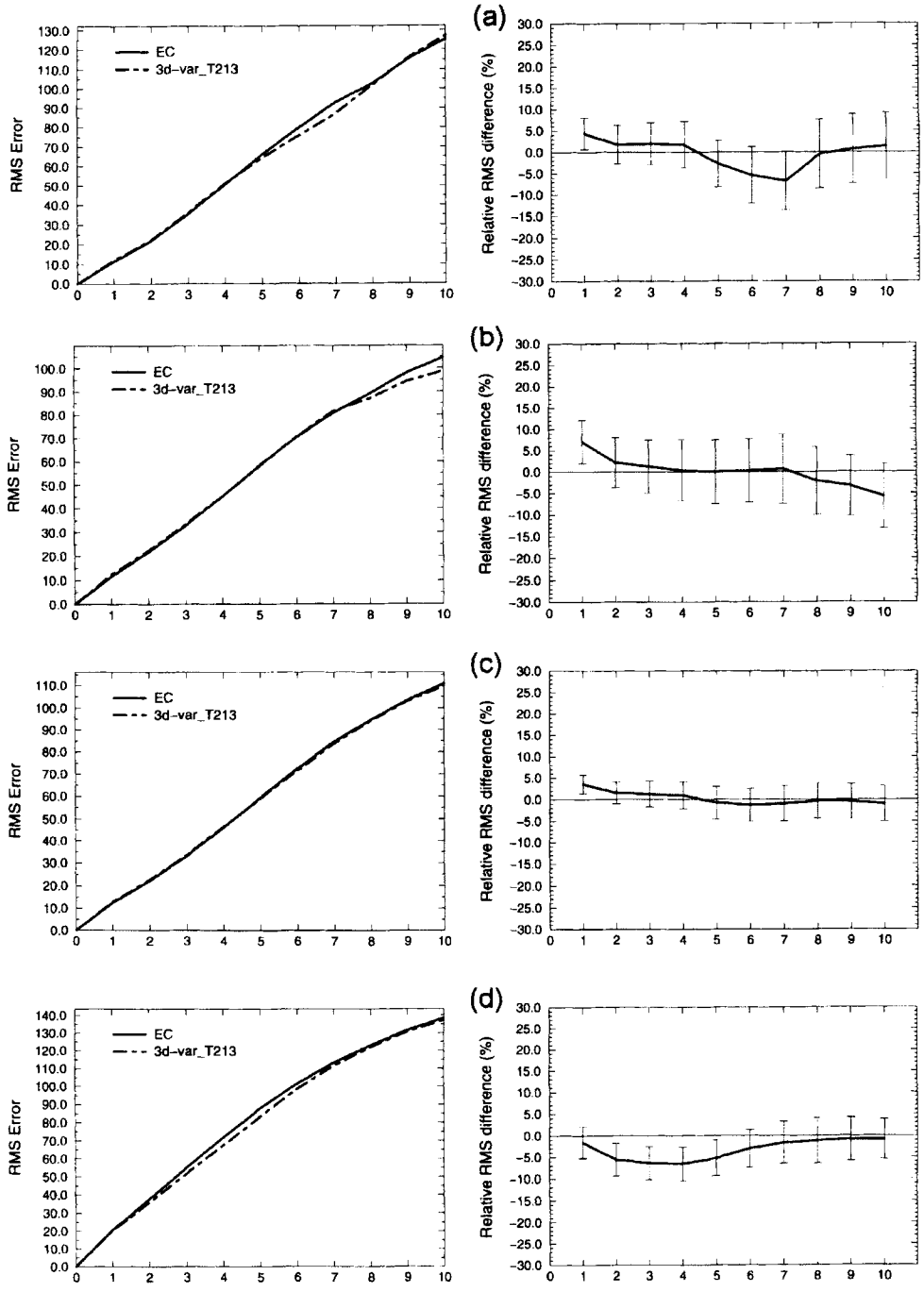

Figure 1. Average scores for forecasts of geopotential at 500 hPa, from 12 UTC on 120 days in three separate periods (5 April 1995–14 May 1995; 24 August 1995–28 October 1995; 16 January 1996–29 January 1996), verified against their own analyses: (a) Europe; (b) North America; (c) northern hemisphere (north of 20°N); (d) southern hemisphere (south of 20°S). The left-hand plot in each panel shows the r.m.s. error (m), and the right-hand plot the relative r.m.s. difference (per cent). The full line denotes OI and the dashed line 3D-Var.

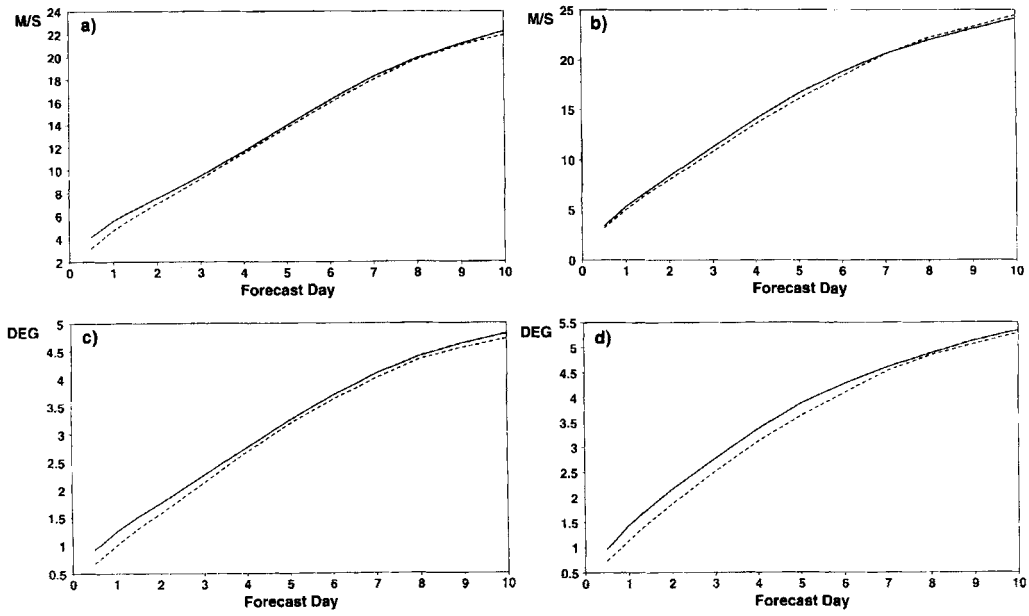

Figure 2. Average r.m.s. errors of forecasts of wind (m s^{-1}) and temperature (K) at 200 hPa, averaged over 120 days at 12 UTC in three separate periods (5 April 1995–14 May 1995; 24 August 1995–28 October 1995; 16 January 1996–29 January 1996), verified against their own analyses: (a) northern hemisphere wind; (b) southern hemisphere wind; (c) northern hemisphere temperature; (d) southern hemisphere temperature. The full line denotes OI and the dashed line 3D-Var.

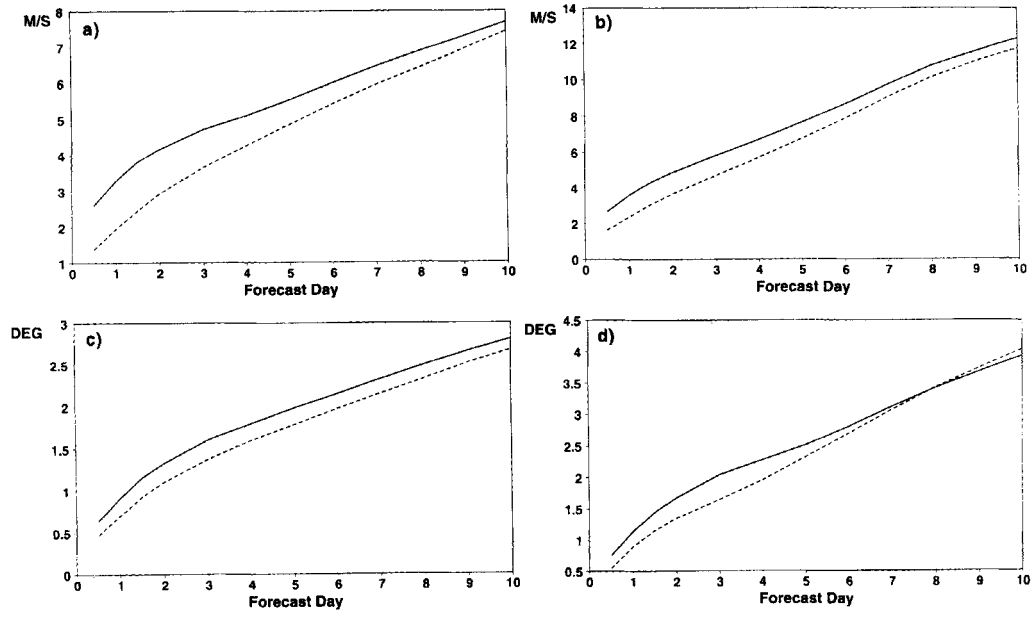

Figure 3. Average r.m.s. errors of forecasts of wind (m s^{-1}) and temperature (K) at 50 hPa, averaged over 120 days at 12 UTC in three separate periods (5 April 1995–14 May 1995; 24 August 1995–28 October 1995; 16 January 1996–29 January 1996), verified against their own analyses: (a) northern hemisphere wind; (b) southern hemisphere wind; (c) northern hemisphere temperature; (d) southern hemisphere temperature. The full line denotes OI and the dashed line 3D-Var.

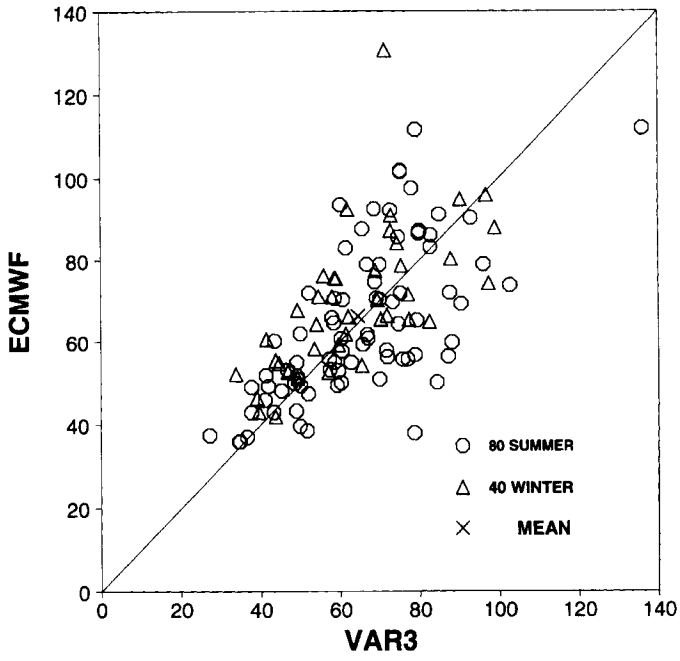

Figure 4. Scatter diagram of r.m.s. error (m) of forecasts of geopotential at 500 hPa for 120 days at 12 UTC in three separate periods (5 April 1995–14 May 1995, 24 August 1995–28 October 1995, 16 January 1996–29 January 1996), for 3D-Var (x-axis) and OI (y-axis). The 40 winter cases are denoted by triangles and the 80 summer cases by circles. The cross indicates the mean.

temperature, wind and geopotential, from 100 hPa and above. In Fig. 3 we show, as an example, the r.m.s. of forecast error of 50 hPa wind ((a) and (b)) and temperature ((c) and (d)) for the two hemispheres. There is a clear improvement over the entire forecast range. The stratospheric analysis will be discussed in subsection 5(d) below.

(*c*) *Case-to-case variability*

The large variability is best illustrated by scatter plots of the type shown in Fig. 4. Here, 3D-Var forecast performance, as measured by the r.m.s. error in forecasts of 500 hPa geopotential (x-axis), is plotted against OI performance (y-axis), each marker representing one 5-day forecast. There are 120 markers in all: circles represent summer cases (May to October) and triangles winter (November to April). The cross represents the mean. The points near, or on, the diagonal represent cases with equal 3D-Var and OI forecast quality. Points above the diagonal indicate cases in which 3D-Var has out-performed OI, and vice versa for points below the diagonal. The figure shows the European area, i.e it corresponds to Fig. 1(a). There is a large number of cases in which one scheme is better than the other, with an approximately equal incidence of poor (and good) forecasts with both schemes. The same is true for all northern hemisphere areas (not shown). In the southern hemisphere, for days 2 to 6, however, there is a significant shift in the cloud of points in favour of 3D-Var (also not shown).

Figure 4 gives the impression of a relatively random variation in forecast performance. However, there was a tendency for poor (good) forecasts to appear in batches over periods of five days or more. To illustrate this we have picked out the best and the worst 14-day periods from the 120-case sample. The two 14-day averages of the r.m.s. forecast error at

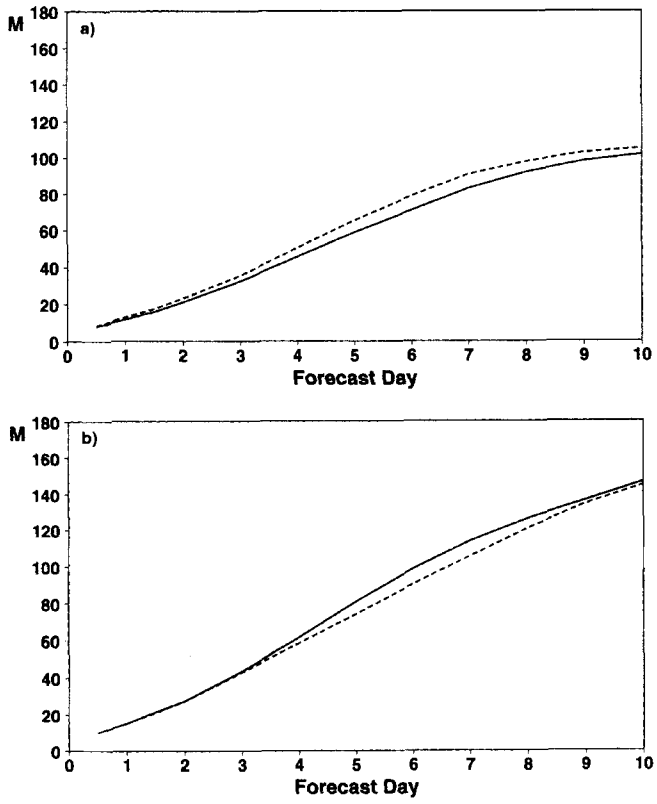

Figure 5. Average r.m.s. error of forecasts of geopotential at 500 hPa for the fourteen-day periods when the 3D-Var performed worst (1 May 1995–14 May 1995) and best (16 January 1996–29 January 1996). The full line denotes OI and the dashed line 3D-Var.

500 hPa are shown in Fig. 5. The bad period (Fig. 5(a)) occurred at the end of experiment B3 (1 May 1995–14 May 1995) and the good period (Fig. 5(b)) is B5 (16 January 1996–29 January 1996). Any conclusions drawn from study of either of these two periods in isolation would be entirely inaccurate. We therefore reiterate the importance for the evaluation of data-assimilation schemes of samples being large enough.

The problem of an adequate size of sample is less acute when looking at the performance of short-range forecasts. It is therefore easier to validate a change to the analysis system with respect to short-range forecasts, but this is not enough. There may be differences between the two schemes in components of the analysis error that grow more slowly and are important for the medium-range performance.

(*d*) *The tropics*

There were repeated changes to the tropical analysis during the experimentation. We therefore restrict the presentation to reflect results obtained with the final configuration only, i.e. experiment B5 and the first two weeks of B4 which were re-run with the final version of 3D-Var. The tropical sample thus comprises 28 cases, 14 in January and 14 in August and September. For the tropics we choose to present forecast verifications against observations rather than against analyses of those observations. This is because in the tropics the latter verification method is quite sensitive to the choice of verifying analysis.

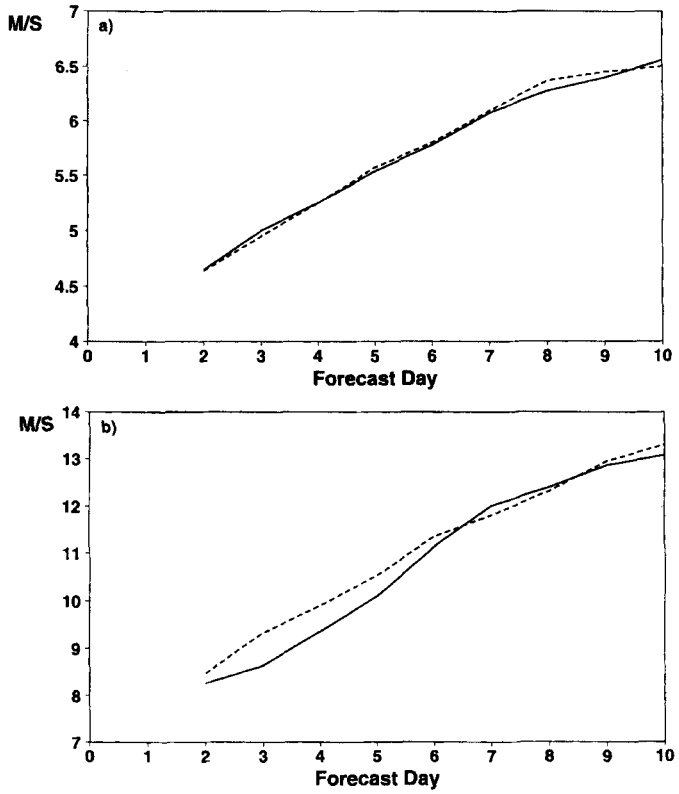

Figure 6. R.m.s. of the differences (m s^{-1}) between forecasts of vector winds from two to ten days ahead and corresponding radiosonde observations, for the tropical region within 20 degrees of the equator. The full line denotes OI and the dashed line 3D-Var.

The forecast verification against observations are shown in Fig. 6 for wind at 850 hPa (a) and 200 hPa (b). We can see that 3D-Var and OI perform equally well at 850 hPa and that OI has an advantage at 200 hPa out to day six. Geopotential scores show an advantage for 3D-Var (not shown). Temperature scores show that 3D-Var is better in the lower troposphere whereas OI is better in the upper troposphere (also not shown).

(*e*) *Summary*

The assimilation and forecast experiments show a neutral impact of 3D-Var with respect to OI, in terms of geopotential in the troposphere of the northern hemisphere extratropics. The scores for wind and temperature show a slight advantage for 3D-Var, while the very-short-range-forecast scores have deteriorated somewhat. The southern hemisphere has improved significantly, whereas there is a mixed result in the tropics. The clearest improvement is in the tropics, and in the stratosphere of both hemispheres.

5. Illustration of 3D-Var characteristics

In order to facilitate the validation of the new scheme, at the outset we intended to use the same observation errors in 3D-Var as in OI and to use a globally averaged set of the OI background-error statistics. It soon became apparent that this strategy was unhelpful

because it compounded the restrictions of the two schemes, i.e. the separability of OI and the global homogeneity of 3D-Var. The direct use of TOVS radiances required a more accurate representation of the temperature background-errors than could be achieved by the separable model (Andersson *et al.*. 1993). So, we decided to derive and implement non-separable background-error statistics for 3D-Var, as presented in Part II, following Parrish and Derber (1992). Some observation errors had to be adjusted, too, (see tables in appendix B of Part I) since those had in some instances been set artificially high (or low) to compensate for deficiencies in the OI background-error formulation.

Part II reported on five very significant improvements brought by the non-separable formulation: the horizontal structures broaden with height in the stratosphere; the geopotential vertical correlations are broader than those for wind; the temperature correlations are broader in the vertical and sharper in the horizontal; the temperature standard errors are smaller, and the wind standard errors in the stratosphere are smaller than used in OI. The filtering properties of the 3D-Var analysis are therefore different from OI. This can be seen from the way analyses fit data (subsection (a) below and three examples illustrating the response to surface pressure data (subsection (b)), AIREP temperature data (subsection (c)) and stratospheric radiosonde data (subsection (d)). The near-surface wind and tropical cyclone analysis is discussed in subsection (e).

(*a*) *Fit to data*

Statistics of the departures of observations from background and first-guess fields are plotted in Fig 7. The figure shows r.m.s. values of observation-minus-background as full line and r.m.s. of observation-minus-analysis dashed, for radiosonde height and u-component wind data, accumulated over a 14-day period. The fit to radiosonde-height data is relatively similar in the two systems (dashed lines show observation minus analysis). Wind data, however, are fitted much more closely by OI than by 3D-Var. The quality of the background is nonetheless similar (full line, showing observation minus background). It appears that the 3D-Var scheme filters the wind data more heavily than OI. This is because the vertical correlations for wind are broader in 3D-Var, especially over data-dense continental areas where OI uses very sharp vertical correlations. The OI structure functions were especially tuned in this manner in order to fit data closely in jet-stream situations (Lönnberg 1989). The effect is most noticeable in data-dense areas such as North America and Europe, where OI fits the data very closely, whereas the 3D-Var filters the data and produces a smoother analysis. It should be remembered that the quality of the background (a six-hour forecast) is similar in the two schemes. This is an indication that some of the closer fit to the observations of OI is in some sense compensated by the better 3D-Var balance, so that short-range forecasts are of similar accuracy.

The stronger smoothing of wind data in data-dense areas is not entirely satisfactory and could contribute to the development of errors in the medium-range forecasts. A set of three 14-day assimilations was run in order to test the sensitivity to the broadness of the 3D-Var structure functions. One experiment used artificially sharpened structure-functions, one used broadened functions and one was the unmodified control. The modifications were obtained by multiplying the autocorrelation spectra by $n^{0.8}$ and $n^{1.5}$ respectively (and renormalizing to obtain correlation spectra, as in Part II, subsection 3(b)), giving sharper/broader structure functions in the vertical as well as in the horizontal. The sharp structure-functions gave a closer fit to wind data and improved the performance of the forecast for the European area (not shown); for the northern hemisphere as a whole, however, differences in performance of the forecast were neutral, and for the southern hemisphere they were very poor. The broad structure functions degraded the results for the northern hemisphere slightly and improved those for the southern hemisphere. The best overall was the control

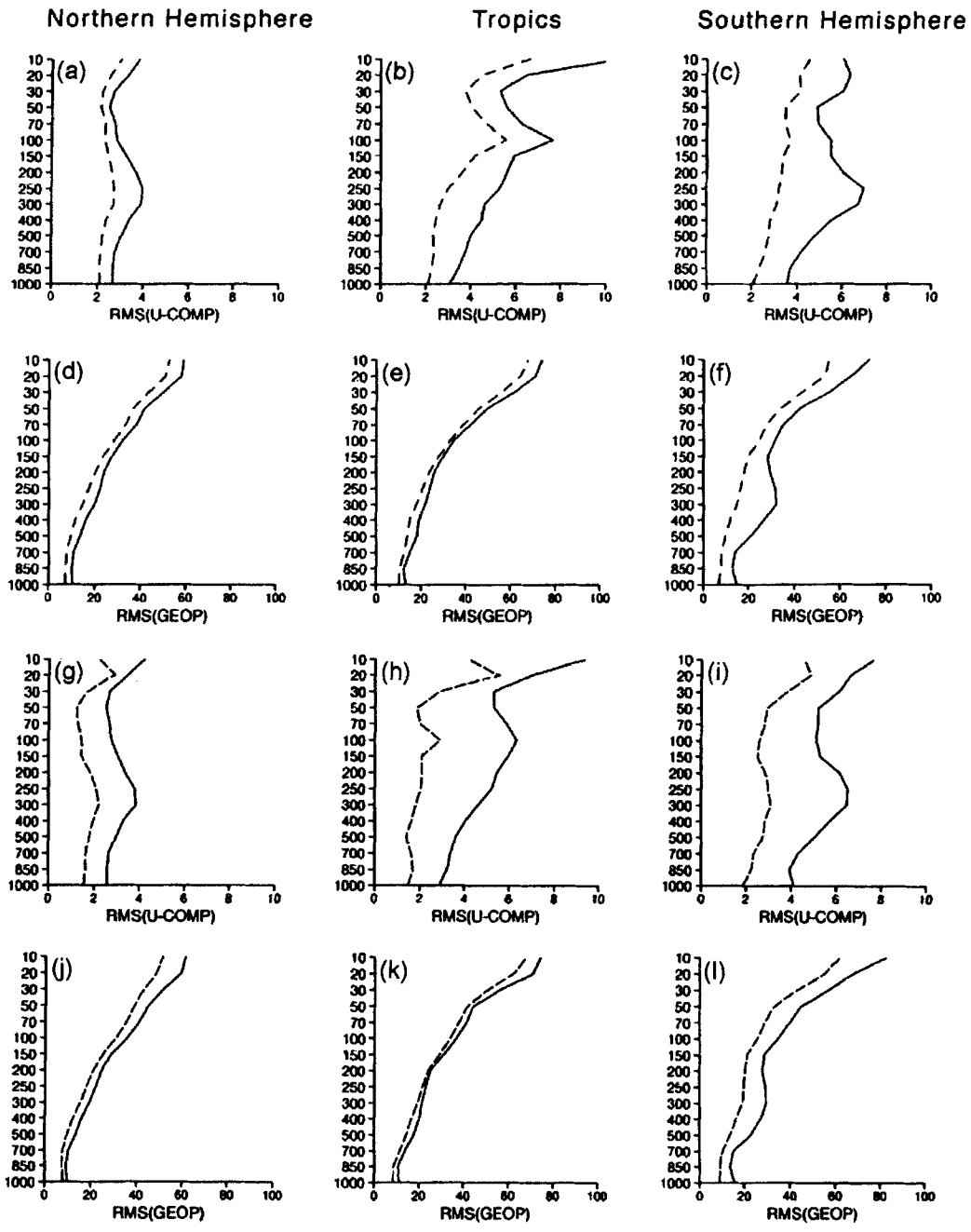

Figure 7. R.m.s. differences at levels from 1000 hPa to 10 hPa for the fourteen-day period 12 UTC 24 August 1995–6 September 1995, between values from all radiosonde data which were used and corresponding values from 3D-Var and OI:

(a) *u* component, 3D-Var, NH; (b) *u* component, 3D-Var, tropics; (c) *u* component, 3D-Var, SH;
(d) geopotential, 3D-Var, NH; (e) geopotential, 3D-Var, tropics; (f) geopotential, 3D-Var, SH;
(g) *u* component, OI, NH; (h) *u* component, OI, tropics; (i) *u* component, OI, SH;
(j) geopotential, OI, NH; (k) geopotential, OI, tropics; (l) geopotential, OI, SH.

NH denotes northern hemisphere north of 20°N, SH denotes southern hemisphere south of 20°S and tropics denotes the region within 20 degrees of the equator. Pecked lines denote observation minus analysis and full lines observation minus background.

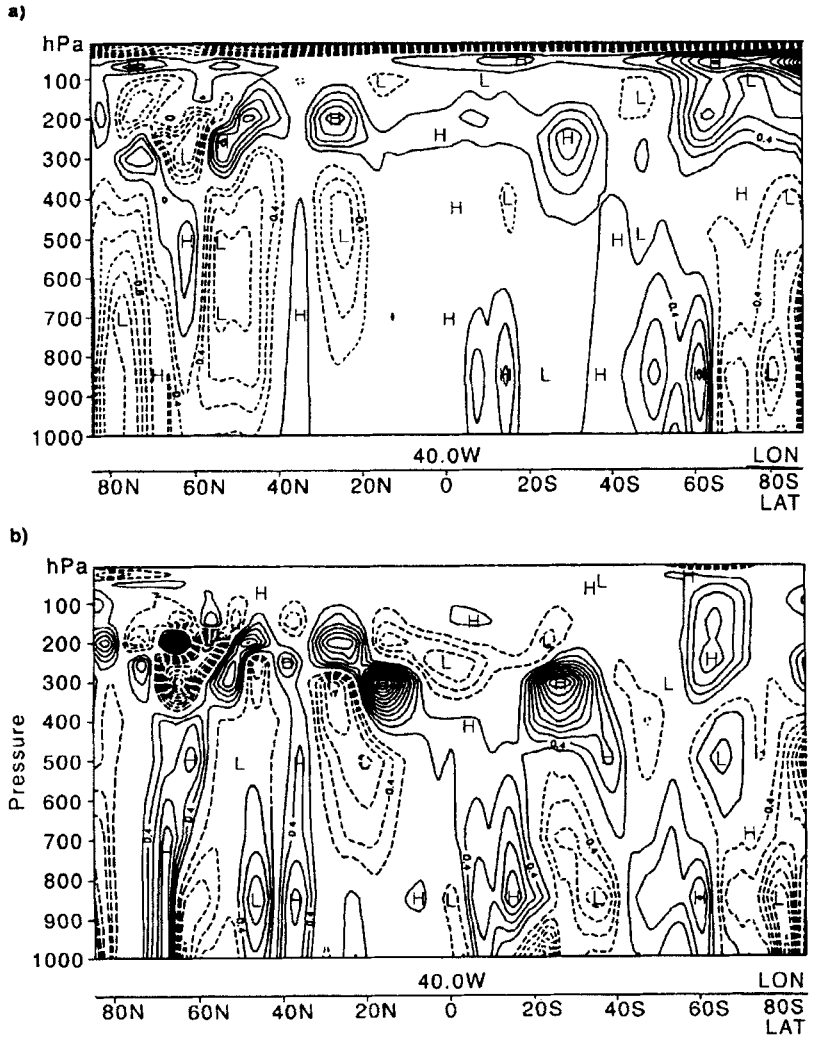

Figure 8. North–south cross-section along 40°W of analysis increments of temperature (K) at 00 UTC 16 August 1993 for analyses without TOVS or SATEM data: (a) 3D-Var; (b) OI. Contour interval 0.2 K.

assimilation. We concluded that geographically varying structure-functions are desirable; this would require a generalization of our present 3D-Var formulation (as discussed in Part I, subsection 3(a)(vi)). These issues are currently subject to further investigation, with the aim of introducing more geographical variation in 3D-Var in the near future.

(*b*) *Response to AIREP temperature data*

The response to temperature data has changed considerably with the introduction of 3D-Var. The OI temperature structure-functions are very sharp in the vertical, with negative lobes either side of the observation. The 3D-Var temperature structure-functions are broader and change sign at about the tropopause level (see Fig. 8(a) of Part II). The temperature horizontal length-scale, however, is shorter in 3D-Var (approximately 300 km) than in OI (500 km). Figure 8 shows temperature cross-sections of 3D-Var (a) and OI (b)

analysis increments, orientated from north to south over the Atlantic Ocean. These analyses have not used TOVS data and there are no radiosonde data affecting the area of interest. The diagrams show the response to AIREP temperature (T) and wind data when used in conjunction with surface-pressure data—a frequent condition over the North Atlantic and the North Pacific. We can see that the AIREP data in OI give rise to increments which are localized between 300 and 100 hPa, and that the surface-pressure data (p_s) produce temperature increments near 850 hPa (as expected from the OI $p_s - T$ cross correlations). There are generally small increments in mid-troposphere. In 3D-Var, on the other hand, these two types of data produce temperature-analysis increments which are more broadly distributed in the vertical and tend to have maxima in mid-troposphere, away from the data. There appears to be an interaction between the AIREP data and the surface-pressure data in 3D-Var, which is absent in the more localized OI analysis. This tendency for broader temperature-analysis increments in 3D-Var is a feature imposed by the specified background-error statistics. It has been explained in Part II that the temperature vertical correlations are unrealistically sharp in OI due to the separability assumption.

The correct structures for the extrapolation of the AIREP temperature information depend strongly on the synoptic situation. The static structure-functions employed in both OI and 3D-Var are both likely to be far from correct in many situations. We know, however, that the 3D-Var temperature correlations are closer to the truth, in a statistical sense. In view of the different response to AIREP temperature data, assimilation experiments were run excluding just these data in both 3D-Var and OI, for a period of fourteen days. The results indicated a neutral impact on the medium-range forecast in both schemes (not shown).

(*c*) *Barotropic component of surface-pressure analysis*

The non-separable analysis gives a broader (sharper) vertical response to larger (smaller) horizontal scales (Fig. 9 of Part II), i.e. it takes into account the tendency for the large-scale components of forecast error to be more barotropic than the small-scale components. This effect can be clearly demonstrated in an analysis of surface-pressure data only. Figure 9 shows the analysis increments in a 3D-Var analysis of surface-pressure data from SYNOP, SHIP, BUOY and PAOB reports. The top panel (a) shows 1000 hPa and the bottom panel (b) shows 300 hPa, in the Antarctic region. Comparing the two plots, we see that the small-scale increment at 100°E has less vertical propagation than the larger-scale increments at 140°E and 160°W. The two increments have similar amplitude at 1000 hPa, but at 300 hPa they differ by a factor of two—the large-scale increment having the larger amplitude. That is to say, the small-scale surface-pressure increment decays with height primarily within the troposphere, whereas the large-scale pattern penetrates into the lower stratosphere. The cross-correlation between surface pressure and temperature (Fig. 9(b) of Part II) confirms this behaviour, as the correlation for high wave-numbers (small scales) is confined to the lower troposphere, whereas for low wave-numbers there is a maximum in the troposphere and a secondary one in the lower stratosphere. This feature of 3D-Var arises from the improved specification of background-error statistics. It appears to be especially important for the use of single-level data in data-sparse areas such as the southern hemisphere oceans.

(*d*) *Stratospheric analysis*

Mid-latitude wind-forecast errors σ_U are related through geostrophy to geopotential-forecast errors σ_P according to the formula $\sigma_U = \sigma_P/(fl_i)$, where f is the Coriolis parameter and l_i is the length-scale of the geopotential-forecast error-correlation spectrum at level i. In a separable analysis scheme (like ECMWF OI) l_i is constant in the vertical

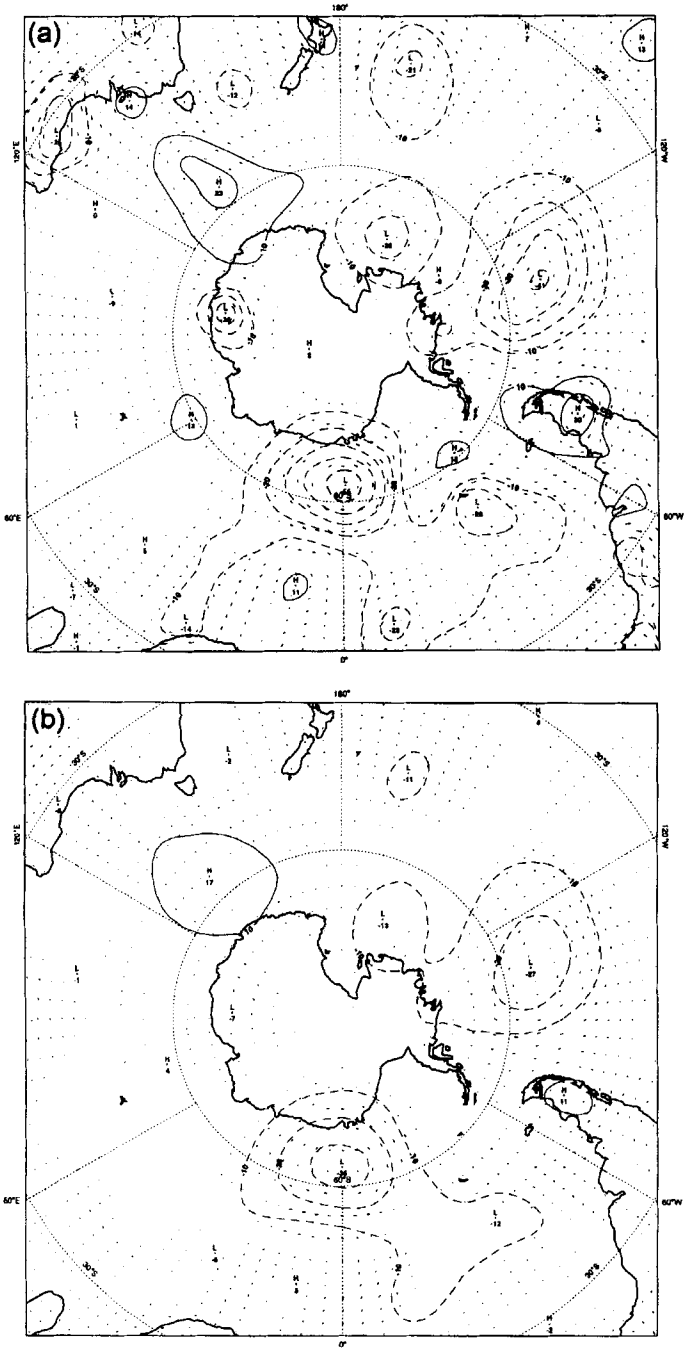

Figure 9. Analysis increments of geopotential height for an analysis using surface-pressure data only (from SYNOP, SHIP, DRIBU and PAOB reports) for southern mid- to high latitudes: (a) 1000 hPa; (b) 300 hPa. Contour interval 10 m; negative contours pecked.

($l_i = 500$ km) which forces σ_U and σ_P to have the same vertical variation. In 3D-Var on the other hand, l_i varies from approximately 500 km in the troposphere to 1000 km at the top of the model, causing σ_U to increase with height less rapidly in the stratosphere than σ_P. This, plus the direct effect of having broader structure functions at higher levels, has a large impact on the stratospheric analysis. The OI analysis has a tendency to fit radiosonde wind-data far too closely in the stratosphere, creating isolated 'bulls-eyes'. This shows most clearly in maps of analysed potential vorticity on isentropic surfaces. Figure 10 shows 3D-Var (top) and OI (bottom) at 475 K.

The indication is that the OI analysis produces dynamically inconsistent structures ('blobs' of potential vorticity) by drawing to the wind observations in an inappropriate way. The benefits of the better 3D-Var analyses are translated to lower medium-range forecast errors in the stratosphere in both hemispheres, as we have seen from Fig. 3.

The improved quality of stratospheric analyses has also been noted in a report from the Danish Meteorological Institute (Knudsen 1996). ECMWF stratospheric analyses were compared with radiosonde measurements made in the Arctic; a marked reduction in bias of layer-mean temperatures was found after the introduction of 3D-Var.

(*e*) *Near-surface wind and tropical cyclone analysis*

The near-surface analysed wind fields have been verified against an independent data-set, namely the ERS-1 altimeter winds. The ERS-1 altimeter produces wind-speed observations every 7 km along the satellite track. In order to obtain comparable scales, the average of 20 successive observations was compared with the analysed wind-speeds. Results for the test period from 8 August 1995 until 5 October 1995 for the southern hemisphere show a reduction in the standard deviation of error of 0.22 m s^{-1}, from 1.99 m s^{-1} in OI to 1.77 m s^{-1} for 3D-Var. A smaller improvement was found in the northern hemisphere, and virtually no change in the tropics. The improvement in near-surface wind has translated into a considerably better quality of first-guess and forecast ocean-wave-height. A comparison of first-guess wave-height produced by the WAM model (Komen *et al.* 1994) with ERS-1 altimeter wave-heights shows a reduction in standard deviation of wave-height error of 10%, from 0.50 m using OI winds to 0.45 m using 3D-Var winds. The anomaly correlation of wave-height forecast in the southern hemisphere suggests an improvement of wave forecast skill (at the 60% level) of about half a day, while from day 3 onwards the standard deviation of wave-height error is reduced by about 5% (not shown). The main part of the improvement is thought to derive from the use of ERS-1 scatterometer wind data in the 3D-VAR analysis.

Figure 11 shows an example of an analysis of a tropical cyclone—in this case tropical cyclone *Karen*, on 31 August 1995. Panel (a) shows the observed scatterometer winds for an orbit which passes directly over the cyclone position (indicated by a large dot, at 20°N, 52°W). Panel (b) shows the background (six-hour forecast) valid at the same time, and panel (c) the 3D-Var analysis. The OI analysis is not shown, but is similar to the background field in this case. This is because few conventional data exist in this area, and ECMWF OI does not use scatterometer wind data. We see that the 3D-Var, when using the ERS-1 winds, has produced a good analysis of the cyclone. In every ERS-1 location, 3D-Var has the choice between two equally probable winds with approximately opposite directions. This very rarely leads to any difficulties; the wind analyses are always horizontally consistent (Gaffard *et al.* 1998).

This is a striking example of the favourable impact of the additional data used in 3D-Var. Statistically, over the whole experiment period we see a significant improvement of the definition of the analysed wind field in and around tropical cyclones. Table 2 shows the result of a subjective study of all reported tropical cyclones (hurricanes, typhoons and

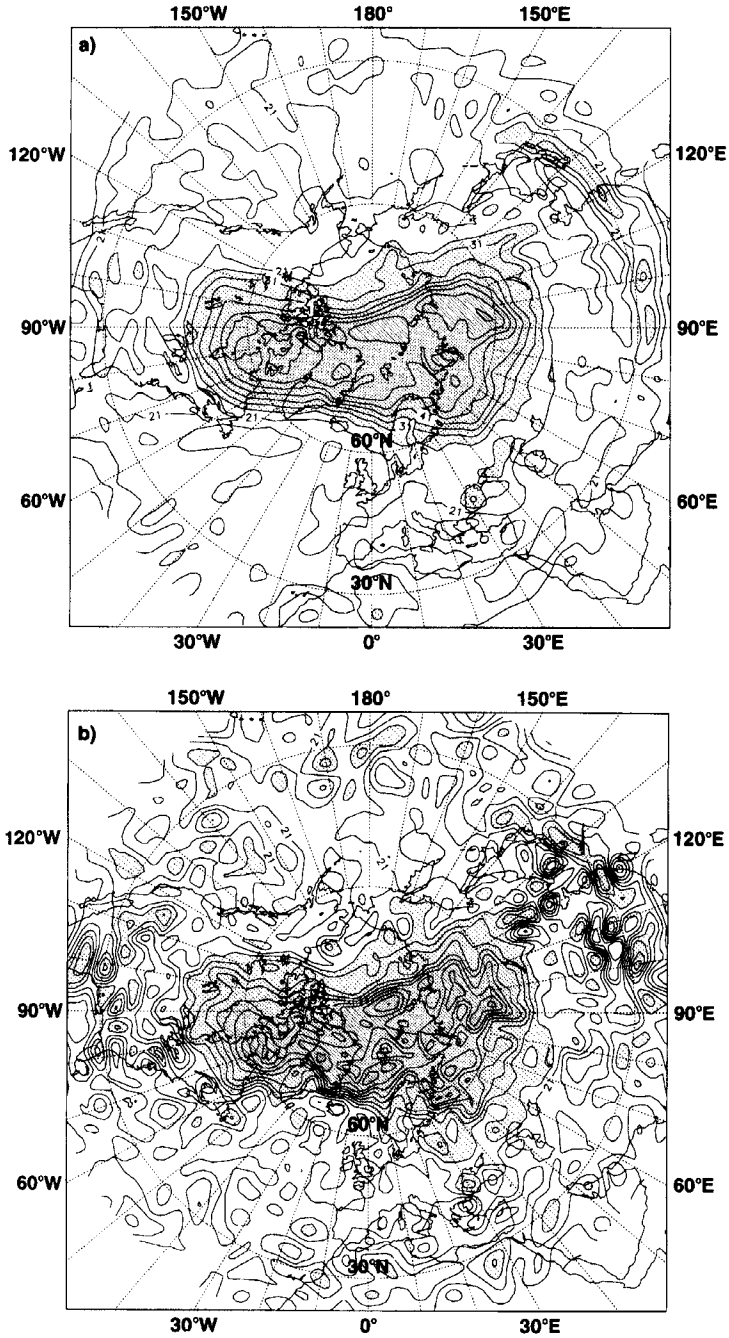

Figure 10. Potential vorticity on the 475 K isentropic surface in northern mid- to high latitudes at 12 UTC 29 January 1996: (a) 3D-Var; (b) OI.

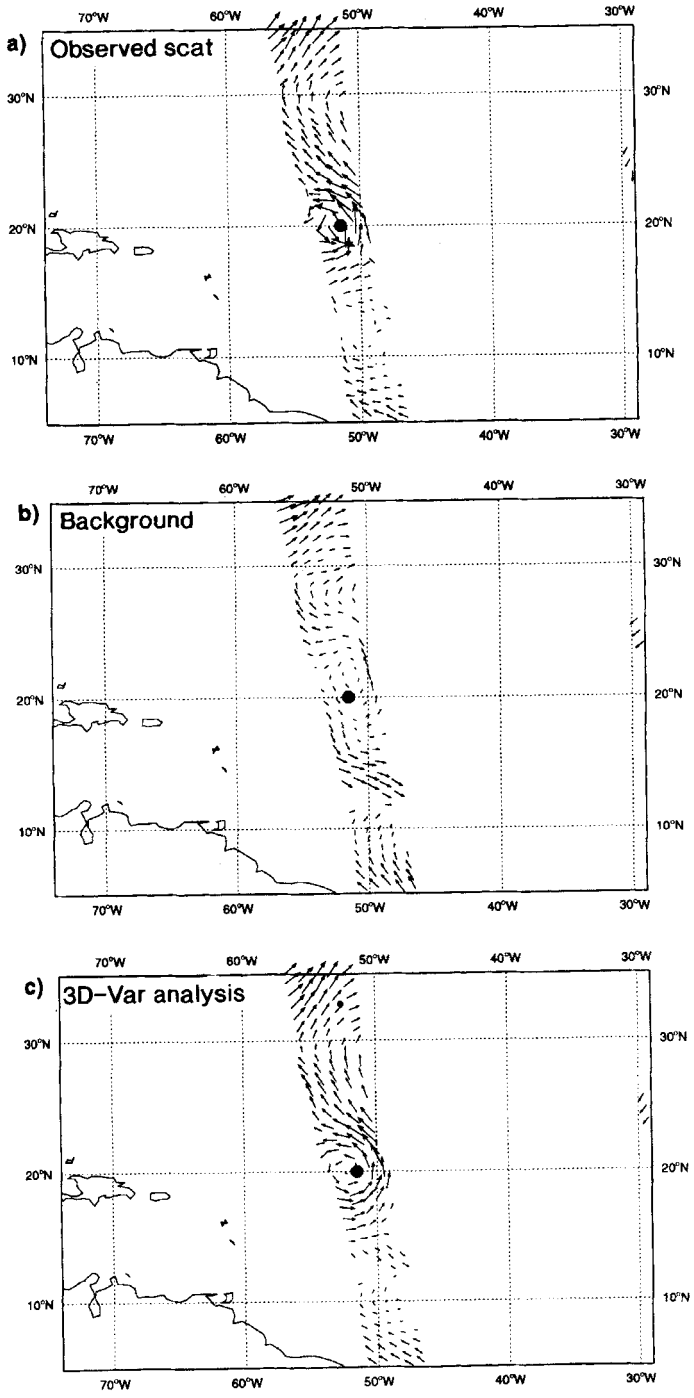

Figure 11. Winds beneath an orbit which passes over tropical cyclone *Karen* located at 20°N, 52°W (large dot) on 31 August 1995: (a) observed by scatterometer; (b) background (six-hour) forecast valid for the same time; (c) 3D-Var analysis. (b) and (c) are interpo;ated to the positions of the scatterometer observations.

TABLE 2. SUBJECTIVE TROPICAL CYCLONE VERIFICATION.

	Analysis	Forecasts			
		Day 1	Day 3	Day 5	Day 7
Improved	29	23	25	16	12
Neutral	30	32	26	32	18
Worse	6	10	14	12	6

Results of a subjective study of tropical cyclone position and intensity in analyses and forecasts, comparing 3D-Var with OI. The sample includes all hurricanes, typhoons and tropical storms in the period from 28 August 1995 to 18 September 1995.

Totals for Days 5 and 7 are less than 65 because it was not always possible to find features corresponding to analysed storms.

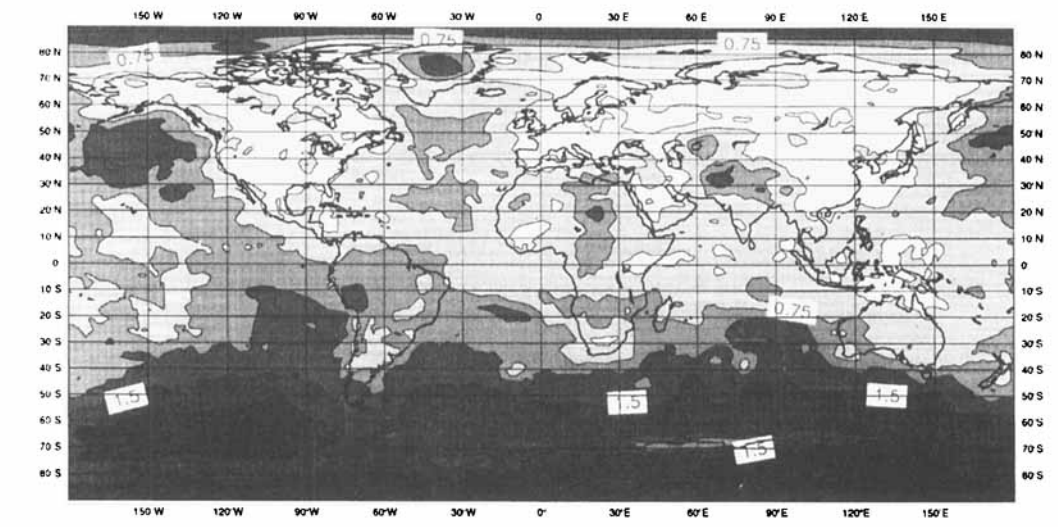

Figure 12. R.m.s. of the difference between 3D-Var and OI analyses of geopotential height at 500 hPa for 120 days at 12 UTC in three separate periods (5 April 1995–14 May 1995; 24 August 1995–28 October 1995; 16 January 1996–29 January 1996). Contours are for 0.3, 0.5, 0.75, 1.0, 1.5 and 2.5 dm. Shading is omitted below 0.5 dm.

tropical storms) in the period between 28 August 1995 and 18 September 1995 comparing the position and intensity of the cyclones in the 3D-Var and OI analyses and forecasts. In a sample of 65 cyclone analyses, 29 were improved, 30 were equal and 6 were worse. The improved analyses led to better forecasts in the short range (day 1 and day3), Table 2. Tomassini *et al.*. (1998) studied all tropical cyclones in the North Atlantic in the (overlapping) period 24 August 1995 to 8 September 1995 and found that the mean positional error in analyses had been reduced from 173 km in OI analyses to 111 km in 3D-Var.

(*f*) *Discussion*

Figure 12 shows root-mean-square of the difference between 3D-Var and operational analyses of 500 hPa geopotential, for the 120 days of B3 to B5. We see that the two analyses generally are very close over the continents in the northern hemisphere (less than 5.0 m r.m.s. difference), and that larger differences (7.5–10.0 m r.m.s.) occur over the Atlantic and Pacific Oceans. The largest differences are, as expected, in southern hemisphere mid-

latitudes (in excess of 15 m) and over the Antarctic, where data are relatively sparse and the analysis least certain.

The two most sensitive areas at initial time for medium-range forecasts for Europe are firstly eastern North Pacific and secondly eastern Canada with the Labrador Sea and adjoining parts of the North Atlantic (Rabier *et al.*. 1996a). The analyses in these areas are mostly influenced by TOVS and single-level data, such as surface pressures from ships, and winds and temperatures from aircraft reports. We have seen from the results in this section that these particular data give rise to significant differences between analyses from 3D-Var and those from OI. This may explain some of the large case-to-case variability in relative forecast skill, reported in section 3.

6. Developments during pre-operational tests

During the pre-operational tests, the team of people scrutinizing the results included the developers of the scheme, together with experts in physical parametrization, diagnostics and operational forecasting. This brought into focus aspects of the new scheme which could otherwise have been overlooked. The investigations revealed important shortcomings in the tropical mass–wind balance, the humidity analysis and model spin-up, and the precise configuration for TOVS-data usage. The resulting developments are presented in this section.

(*a*) *Tropical mass–wind balance*

The tropical mass–wind balance is imposed by the J_b term of the 3D-Var objective function. The control variable is split into two parts, a balanced and an unbalanced one, defined by a projection onto the Hough modes of the model (see Part I, subsection 3(d)). The desired degree of balance is achieved by explicitly assigning different weights to the two parts.

In experiments B1 to B3, a multivariate formulation was used. It produced balanced analysis increments which were retained by initialization. In the multivariate formulation some serious problems affecting the wind analysis emerged. Figure 13(a) shows the mean analysis increments of surface pressure for the South American region, averaged over 14 days (from 21 April to 14 May 1995), all at 18 UTC, approximately local noon. We see average positive increments over most of the Amazon basin, with a maximum of 2.0 hPa. The existence of these increments indicates a systematic model under-estimation of the surface pressure at local noon. With the multivariate formulation, 3D-Var produced strong wind-increments on the same regional scale to balance the mass increments, Fig. 13(b). The resulting wind analysis is not in agreement with near-surface wind observations (not shown) and therefore erroneous.

A recent paper by Daley (1996) demonstrated that formulations based on the application of the linear balance-equation or a Rossby–Hough expansion imply a tropical coupling between the mass and rotational wind forecast errors which does not seem to exist in reality. Daley constructed a filtered form of the linear balance-equation which was essentially uncoupled in the tropics, and closer to reality. This explains our difficulties with the balanced formulation. As described in Part I (subsection 3(d)) a univariate formulation was developed. Like ECMWF OI, it produces virtually zero wind-increments in response to mass data (and vice versa) on (or very close to) the equator, gradually becoming more geostrophic further away from the equator. The scheme is fully multivariate poleward of 30°N and 30°S.

The behaviour of the univariate formulation of 3D-Var in the tropics is very similar to OI, as expected. A large part of the mass increments is rejected by initialization and the

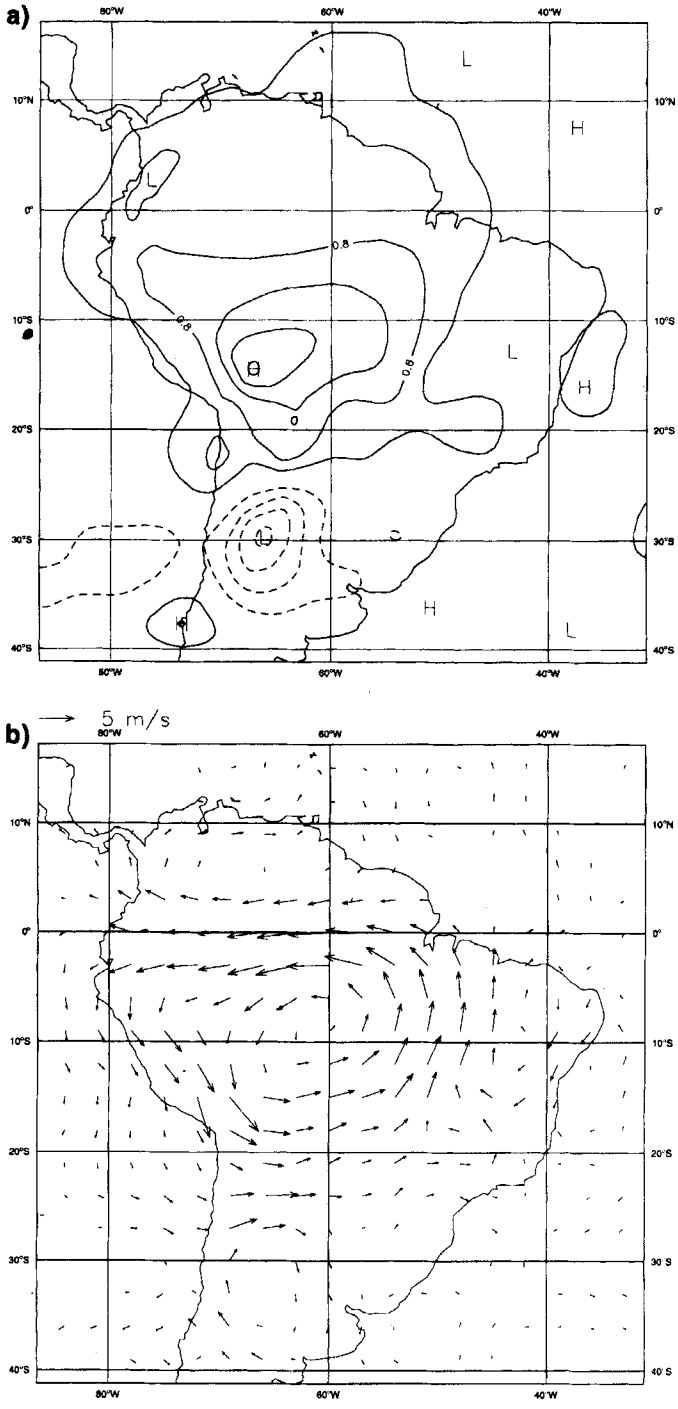

Figure 13. Mean 3D-Var analysis increments over South America at 18 UTC for the fourteen-day period from 21 April 1995 to 4 May 1995: (a) surface pressure (contour interval 0.4 hPa, zero contour suppressed and negative values pecked); (b) vector wind (scale arrow denotes 5 m s^{-1}).

appearance of some noise in the vertical profiles of temperature, near the top of the model, is inevitable.

(*b*) *Humidity analysis*

The analysis variable of the 3D-Var humidity analysis is specific humidity. The main data for the humidity analysis are radiosonde specific humidity, SYNOP two-metre relative humidity and TOVS radiances in channels HIRS-10, 11 and 12. Several other TOVS channels also have a weak dependency on humidity, which is taken into account. There can also be a weak influence on the humidity analysis from surface pressure data and radiosonde geopotential-data through the virtual-temperature effects of the hydrostatic equation (Appendix A of Part I).

(i) *Humidity affected by geopotential data.* One problem of the humidity analysis was the appearance of large positive analysis increments at the lowest model-levels, over some subtropical land areas (Saudi Arabia, North Africa, Mexico and the southern United States), at local midday. These areas are characterized by high temperatures and dry conditions. The moistening could be as high as 5 g kg^{-1} and was at variance with most available humidity data. Investigations showed that these humidity increments occurred at radiosonde locations and were caused by geopotential observations rather than humidity data. Figure 14 shows the resulting mean two-metre specific humidity over the Arabian Peninsula and the mean error at selected SYNOP stations. The plotted numbers represent mean differences between the 3D-Var analyses and observations of two-metre specific humidity, in the period from 1200 UTC 24 August 1995 to 1200 UTC 29 August 1995. The analysis error is between 4 and 10 g kg^{-1} (too moist) at several SYNOP stations in northern and central Saudi Arabia.

We have seen that geopotential data can be fitted by changing both temperature and humidity. In the absence of any other data, the relative changes of humidity and temperature when fitting geopotential data are governed by the background-error standard deviations (of temperature and humidity). The conclusion was therefore that there was a problem with the specification of humidity background-errors (σ_q) in hot and dry conditions. 3D-Var at the time used a background specification of $\sigma_q = 0.15\, q_s(T, p)$ i.e. 15 % of saturation specific humidity. At relatively high temperatures, e.g. 305 K, this gives a background error of almost 5 g kg^{-1}. The findings led to the modified specification given in Part II section 4. An easier but less correct solution would have been to disable the dependency on humidity of the geopotential observation operator. This would, however, produce inconsistencies between the humidity analysis and the geopotential data. The possibility for multivariate observation operators allows 3D-Var to use data more accurately, provided background errors and observation errors are accurately specified.

(ii) *Spin-down.* A second problem of the 3D-Var humidity analysis was a marked spin-down of the tropical convection during the first six hours of forecasts starting from 3D-Var analyses. There was more six-hour precipitation than with OI. One suspicion was that the analysis increments over tropical and subtropical oceans were too large and that a too vigorous redistribution of the tropical humidity by the analysis contributed to the excessive precipitation. Study of radiosonde-minus-model humidities gave an indication that the humidity background-errors should be reduced in the tropical oceanic boundary-layer. This resulted in the formulation given in Part II, section 4, but did not solve the spin-down problem. Later, it was discovered that some relatively small volumes of supersaturation were present in the 3D-Var analyses. In the incremental 3D-Var (Part I, subsection 5(a)) the final analysis is created by adding the low-resolution analysis increments to the high-resolution background. This was done without checking for supersaturation (or negative

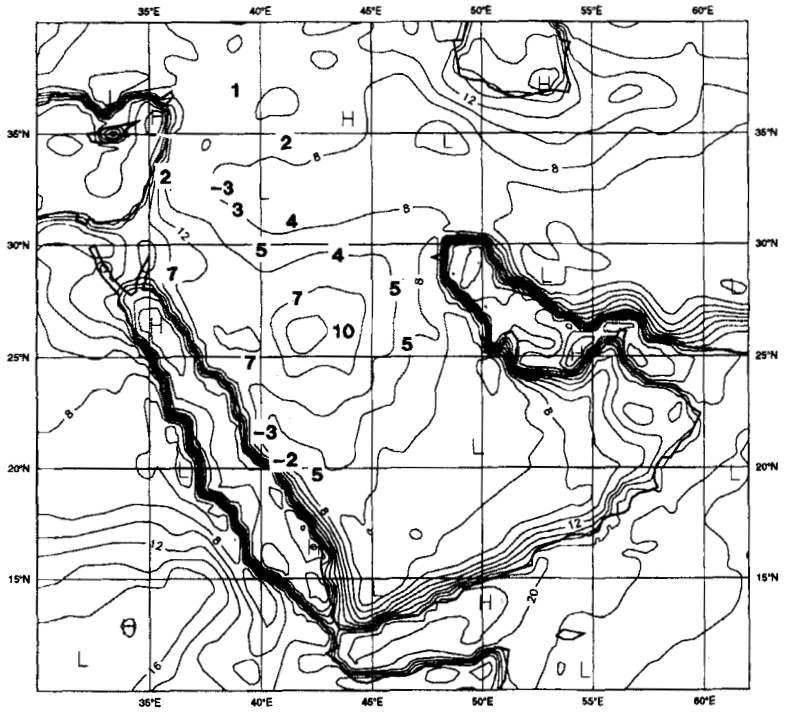

Figure 14. Mean of 3D-Var analyses of specific humidity at 2 m above the surface of the Middle East at 12 UTC from 24 August 1995 to 29 August 1995. Contour interval 2 g kg^{-1}. Numbers in bold show the mean difference between values of specific humidity derived from the analyses and those observed at selected SYNOP stations.

humidity). When this was rectified, the spin-down problem was reduced. Figure 15 shows an example of the time evolution of precipitation in forecasts from OI, uncorrected 3D-Var, and 3D-Var after modification of the humidity analysis. The spin-down problem is clearly visible in the uncorrected 3D-Var. The corrected 3D-Var is more similar to OI.

(iii) *Stratospheric humidity.* A third problem with the 3D-Var humidity analysis occurred in the stratosphere. There are no in situ or satellite humidity data used in the stratosphere. Monitoring of the stratospheric humidity revealed a slow but systematic linear increase with time. The globally averaged humidity above 100 hPa increased from 2.5 10^{-6} to 3.5 10^{-6} kg kg^{-1} during a period of 45 days. The forecast model has not been seen to show this systematic behaviour in long runs. Investigations showed that the analysis introduced small, but generally positive, humidity analysis increments in the stratosphere at each analysis. The mechanism behind the problem turned out to be small, but non-zero, vertical correlations between troposphere and stratosphere, which allowed the systematic component of the tropospheric increments to spread into the stratosphere. The solution implemented was to set the vertical correlations between the levels above 100 hPa and all other levels to exactly zero and to set the background error above 150 hPa to a very small value (1.25 10^{-8} kg kg^{-1}).

(*c*) *TOVS data usage*

The precise configuration of TOVS-data usage is a product of many years of experimentation—first with NESDIS retrieved data, later using 1D-Var retrieved data in OI

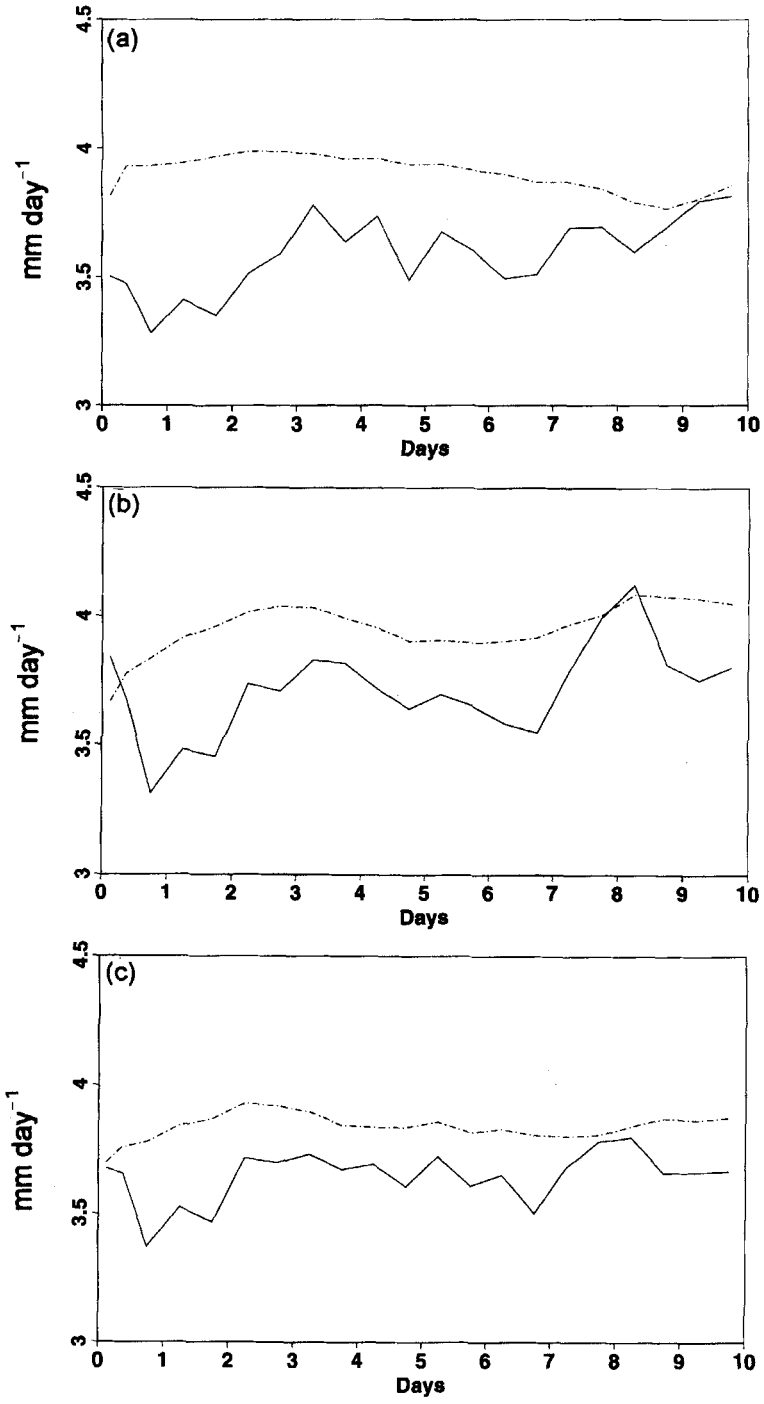

Figure 15. Evolution of precipitation (full line) and evaporation (pecked line) at model points over the sea during forecast periods of up to ten days, from: (a) OI; (b) uncorrected 3D-Var; (c) 3D-Var after modification of the humidity analysis, as later incorporated in the operational model.

and finally using a combination of radiances and retrieved data in 3D-Var. The original intention was simply to use radiances everywhere on the globe instead of retrieved thicknesses, restricting the set of radiances to surface-insensitive channels over land and to cloud-insensitive channels where clouds were detected. This strategy was modified as a consequence of the results obtained by Kelly (1993) who pointed out difficulties in using radiances in the stratosphere. The top of the ECMWF model is currently at 10 hPa, whereas many TOVS channels have a significant contribution from radiation above this level. Kelly found that extrapolation errors caused analysis errors in the upper stratosphere. Assimilations using NESDIS retrieved thicknesses above 100 hPa did not have this problem. The set of radiances for use in 3D-Var was thereby reduced to those that could be described as being predominantly 'tropospheric', and NESDIS retrieved thicknesses were introduced in the extra-tropics between 100 hPa and 10 hPa. This closely mimics the TOVS-data usage of ECMWF OI from December 1995 onwards (McNally and Vesperini 1996). There are plans to extend the model higher into the stratosphere and at that point the TOVS-data usage will need to be readdressed.

In one of the test periods, a 10 K temperature-difference (between 3D-Var and OI) appeared in the lower stratosphere in the Arctic region. It was not obvious which of the two analyses was more correct. Experiments were run excluding some Arctic radiosonde stations to be used for verification. The results were inconclusive. However, forecasts from the 3D-Var analyses rapidly adjusted the Arctic temperatures to produce values close to those of the OI analyses. Further experimentation followed, replacing the radiances in the Arctic region, north of 70°N, with 1D-Var retrieved thicknesses. As a result the difference between the 3D-Var and OI analyses became small enough for this to become the solution for implementation. A better description of the Arctic background-error, in particular a temperature vertical correlation matrix reflecting the low tropopause, may be necessary for the reintroduction of radiances to this area.

7. Conclusions and future directions

A three-dimensional variational analysis scheme (3D-Var) was implemented on 30 January 1996 at ECMWF, replacing OI (Optimal Interpolation). In this set of three papers we have presented the formulation of the new scheme (Part I), the specification of structure functions (Part II) and the results from pre-operational experimentation (Part III).

(*a*) *Summary*

3D-Var uses a wide variety of meteorological data to produce global analyses of temperature, vorticity, divergence, specific humidity and surface pressure, directly on model levels using the model's spectral representation. The global analysis problem is solved simultaneously for all analysis variables by iteratively minimizing the variational objective function. The objective function consists of three terms controlling the distance to the background (a six-hour forecast), the distance to the observations and the norm of the gravity-wave tendency respectively.

The background term includes a coupling between mass and wind. The coupling is achieved by separating the balanced part of the analysis increments from the un-balanced, through a projection on the model's Hough modes. The objective function for the unbalanced part is given a higher weight (corresponding to a lower variance) than the balanced part, which results in predominantly balanced analysis increments. The tropical analysis is univariate.

The observation term includes all observations used by the OI scheme plus the addition of scatterometer wind data. The scheme uses TOVS cloud-cleared radiances instead of

retrieved data in the troposphere, whereas retrieved layer-mean temperatures are retained in the extratropical stratosphere above 100 hPa and in the Arctic. The data are related to the analysis variables through so-called observation operators, which can be multivariate and nonlinear. This makes the scheme very flexible in terms of data usage, and facilitates the introduction of new types of data. This has been explored in the use of TOVS radiances and in the use of directionally ambiguous scatterometer winds. Several projects are underway, aimed at including additional observational data in 3D-Var, e.g. SSM/I products, TOVS raw (as opposed to cloud-cleared) radiances, water-vapour winds and radiances from geostationary satellites. Additional scatterometer winds will also become available in the near future. These data are likely to improve principally the analysis of the tropical wind field and the analysis of humidity.

A non-separable formulation of structure functions is used. This allows the horizontal length-scale to vary in the vertical. It also results in shorter length-scales for temperature than for geopotential and in vertically sharper correlation-structures for wind than for mass. We have demonstrated that the structure-function specification has a profound impact on the analysis increments, particularly with respect to single-level data such as aircraft data and surface pressure observations. The current formulation is globally homogeneous. This is believed to be the cause of some 3D-Var analysis deficiencies in the tropics and in the polar regions.

The pre-operational tests at full operational resolution (T213) comprise a very large number of cases—in total 163 days, in five separate periods. This extensive experimentation was necessary because of a very large variability in forecast performance between the two schemes. In some periods 3D-Var performed clearly better than OI, in other periods the situation could be the reverse. These variations are very difficult to interpret, and for now have to be seen as random variations in the relative performance of the two schemes. We showed that samples greater than fifty cases were required for reliable estimation of mid-latitude forecast impact. We averaged the 120 cases run after an important model change (the prognostic cloud-scheme). On average over those 120 cases we found a neutral impact in the northern hemisphere extratropics in terms of geopotential, whereas wind and temperature scores were positive. In the southern hemisphere there was a significantly positive impact in terms of geopotential, wind and temperature. The tropical results were mixed. The main areas of difficulty during the pre-operational tests have been discussed in section 6 of this paper. They include the tropical mass–wind balance, several aspects of the humidity analysis and the precise usage of TOVS and SATEM data.

The stratospheric analyses are significantly better in 3D-Var, as seen from analysed potential vorticity for example. The 3D-Var structure functions are a better description of the true background errors in the stratosphere, displaying the characteristic increase in horizontal length-scale with height which is not present in OI. The benefits of the better 3D-Var analyses are translated to lower medium-range forecast-errors in the stratosphere, in both hemispheres. There is, nevertheless, undoubtedly scope for further improvement of the stratospheric analyses and forecasts.

The analysis of tropical cyclones has improved by the addition of scatterometer wind data. It has been shown that the mean positional error in analyses of North Atlantic tropical cyclones has been reduced from 173 km in OI to 111 km in 3D-Var (Tomassini *et al.*. 1998). The improved analyses also led to better forecasts in the short range.

(*b*) *Current directions of work*

The implementation of 3D-Var reported on in this paper relied on the OI scheme for quality control of the data and to calculate standard deviations of background error. The dependence on the OI scheme has, however, recently been removed. The quality control has

been embedded within the variational analysis itself (Andersson 1996) using the method described by Lorenc and Hammon (1988) and Ingleby and Lorenc (1993), and applied to a simulated LIDAR data-set in a two-dimensional variational analysis by Dharssi *et al.*. (1992). We are now applying their technique to the global set of real observations. Results have shown that variational quality control is an adequate and efficient replacement for the traditional OI quality control. The checks against the background fields (the so called first-guess check) have also been replaced by a new module which does not rely on the OI codes.

The replacement for the OI calculation of standard deviations of background error is a two-part procedure which first estimates standard deviations of analysis error and then applies a simple error-growth model (Savijärvi 1995) to estimate standard deviations of background error for the next analysis cycle. The standard deviations of analysis error are estimated using a low-rank approximation based on the leading eigenvectors of the Hessian matrix of the cost functional (Fisher and Courtier 1995).

The mass–wind balance is currently defined through a Hough-mode separation. Two deficiencies of this formulation have been discussed in the present paper. Firstly, the mass–wind balance is not part of the change of variable transformation. This worsens the conditioning of the problem severely unless the same background-error statistics are used for both the balanced and the unbalanced parts of the control variable. In practice we are forced to use the same correlations for vorticity as for divergence, although the results in Part II have indicated that this is a poor approximation. Secondly, the need to uncouple the mass and wind analyses in the tropics leads to the introduction of a transition zone in the subtropics which is fairly arbitrarily defined, at present. It was felt that these known deficiencies to the formulation were not severe, and could be left until after the first operational implementation. Work addressing these problems is now well under way. It involves a reformulation of the background term (Bouttier *et al.*. 1997), based on a statistically modified linear balance-equation. Results so far are promising, and there is scope for further improvements of the scheme in the future.

The current 3D-Var specification of background errors assumes non-separability and global homogeneity, while OI assumes separability and has regional variation of the vertical correlations. In this paper we have stressed the advantages of non-separability and we have demonstrated the disadvantages of not having regional variation. Work is now progressing on introducing such regional variation in 3D-Var. There is ample evidence that there are geographical variations in the vertical correlations of background errors: the temperature and wind error structures are sharper in the tropics and subtropics than in the global average (Part II, Fig. 12); the variation of tropopause height with latitude makes the global average correlations less appropriate at high latitudes (Kelly 1993); there are important differences between data-rich and data-sparse areas (Lönnberg 1988). In a grid-point analysis, it is straightforward to define the vertical background-error correlations in grid-point space with the required geographical variability—as was done in OI. In spectral 3D-Var, however, it is more difficult. Nevertheless, it has been shown that, with some restrictions, it is possible to modify the 3D-Var correlation model locally in grid-point space (Part I, subsection 3(b)). This is done by distorting the vertical geometry of the model in an ad hoc way. The method has been implemented for testing in 3D-Var, with encouraging preliminary results. It is believed that it will improve the realism of the vertical structure-functions in 3D-Var. The possibility of having variable horizontal length-scales, along the lines of the ideas presented in section 3(a)(vi) of Part I, will also be explored.

We have started studying the effects of increased vertical resolution of the stratosphere, and an extension of the model to 0.5 hPa. The vertical extension of the model is important for the assimilation of some relatively high-peaking TOVS channels. We shall also be

looking at the benefits that can be derived from including ozone as a variable in the data assimilation system.

(*c*) *Future developments*

A four dimensional variational assimilation (4D-Var) system relying on this 3D-Var formulation is now being tested. 4D-Var includes the time dimension in the analysis step of the assimilation. It minimizes an objective function measuring the misfit between a model trajectory and the available information (observations and background). Assuming the model is linear, this temporal generalization of 3D-Var produces the same result at the end of the assimilation cycle as the Kalman filter, provided the model is perfect. As a consequence, it uses flow-dependent structure-functions within each assimilation cycle, as illustrated by Thépaut *et al.*. (1996). Recent results have shown good mid-latitude performance of a 4D-Var system on a 6-hour assimilation window (Rabier *et al.*. 1996b). It is hoped that such a system can be implemented operationally in the near future.*

Although the 4D-Var system generates flow-dependent structure-functions within the assimilation period, the structure functions assumed for the background are the same as in 3D-Var. A simplified Kalman filter, currently under development, extends the 4D-Var system to include flow dependence in the specification of the background term of the cost function. The basic formulation was described by Courtier (1994).

Acknowledgements

We are very grateful to Otto Pesonen who ran all the T213 3D-Var experiments as part of the ECMWF parallel suite, and Brian Norris who verified the forecast results against analyses and observations. The foundations of 3D-Var were laid by Jean Pailleux, William Heckley, John Eyre and others, whereas Francois Bouttier, John Derber, Lars Isaksen, Michael Fisher, Heikki Järvinen, Anthony McNally, Sami Saarinen and Roger Saunders have contributed to more recent developments. We are also grateful to all those Météo-France and ECMWF staff who have participated in the IFS–ARPEGE collaboration, in particular Patrick Moll, Philippe Caille, Clive Temperton and David Dent. The graphics were skillfully improved by Jocelyn Williams.

References

Andersson, E. 1996 'Implementation of variational quality control'. Pp. 633–643 in proceedings of ECMWF Workshop on 'Non-linear aspects of data assimilation', 9–11 September 1996. (Available from ECMWF, Reading, UK)

Andersson, E., Hollingsworth, A., Kelly, G., Lönnberg, P., Pailleux, J. and Zhang, Z. 1991 Global observing system experiments on operational statistical retrievals of satellite sounding data. *Mon. Weather Rev.*, **119**, 1851–1864

Andersson, E., Pailleux, J., Eyre, J. R., McNally, A.P., Kelly, G. A., Courtier, P. and Rabier F. 1993 'Assimilation of satellite data by 3D-Var at ECMWF'. Pp. 167–188 in proceedings of ECMWF seminar on 'Developments in the use of satellite data in numerical weather prediction', 6–10 September 1993, ECMWF Reading, UK

Andersson, E., Pailleux, J., Thépaut, J.-N., Eyre, J., McNally, A. P., Kelly, G. and Courtier, P. 1994 Use of cloud-cleared radiances in three/four-dimensional variational data assimilation. *Q. J. R. Meteorol. Soc.*, **120**, 627–653

Bouttier, F., Derber, J. and Fisher, M. 1997 'The 1997 revision of the J_b term in 3D/4D-Var'. ECMWF Tech. Memo. 238, ECMWF, Reading, UK

* Footnote added in press: The 4D-Var system replaced the 3D-Var system operationally at ECMWF from 25 November 1997.

Cardinali, C., Andersson, E., Viterbo, P., Thépaut, J.-N. and Vasiljević, D. 1994 'Use of conventional surface observations in three-dimensional variational data assimilation'. Tech. Memo. 205, ECMWF, Reading, UK

Courtier, P. 1994 'Introduction to numerical weather prediction data assimilation methods'. Pp. 189–207 in proceedings of ECMWF seminar on 'Developments in the use of satellite data in numerical weather prediction', 6–10 Sept. 1993, ECMWF, Reading, UK

Courtier, P. and Talagrand, O. 1987 Variational assimilation of meteorological observations with the adjoint vorticity equation. II: Numerical results. *Q. J. R. Meteorol. Soc.*, **113,** 1329–1347

Courtier, P., Andersson, E., Heckley, W., Pailleux, J., Vasiljević, D., Hamrud, M., Hollingsworth, A., Rabier, F. and Fisher, M. 1998 The ECMWF implementation of three dimensional variational assimilation (3D-Var). I: Formulation. *Q. J. R. Meteorol. Soc.*, **124,** 1783–1807

Daley, R. 1996 Generation of global multivariate error covariances by singular-value decomposition of the linear balance equation. *Mon. Weather Rev.*, **124,** 2574–2587

Dharssi, I., Lorenc, A. C. and Ingleby, N. B. 1992 Treatment of gross errors using maximum probability theory. *Q. J. R. Meteorol. Soc.*, **118,** 1017–1036

Eyre, J. R., Kelly, G. A., McNally, A. P., Andersson, E. and Persson, A. 1993 Assimilation of TOVS radiance information through one-dimensional variational analysis. *Q. J. R. Meteorol. Soc.*, **119,** 1427–1463

Fisher, M. and Courtier, P. 1995 'Estimating the covariance matrices of analysis and forecast error in variational data assimilation'. Tech. Memo. 220, ECMWF, Reading, UK)

Gaffard, C. and Roquet, H. 1998 Impact of the ERS-1 scatterometer wind data on the ECMWF 3D-Var assimilation system. Tech. Memo. 217, ECMWF, Reading, UK

Ingleby, N. B. and Lorenc, A. C. 1993 Bayesian quality control using multivariate normal distributions. *Q. J. R. Meteorol. Soc.*, **119,** 1195–1225

Jakob, C. 1994 'The impact of the new cloud scheme on ECMWF's integrated forecasting system (IFS)'. Pp. 277–294 in proceedings of ECMWF/GEWEX workshop on 'Modelling, validation and assimilation of clouds', 31 October–4 November 1994, ECMWF, Reading, UK

Kelly, G. 1993 'Some aspects of stratospheric data assimilation at ECMWF'. Pp. 271–315 in proceedings of ECMWF workshop on 'Stratosphere and numerical weather prediction', 15–17 November 1993, ECMWF, Reading, UK

Knudsen, B. M. 1996 Accuracy of arctic stratospheric temperature analyses and the implication for the prediction of polar stratospheric clouds. *Geophys. Res. Lett.* **23,** 3747–3750

Komen, G. J., Cavaleri, L., Donelan, M., Hasselmann, K., Hasselmann, S. and Janssen, P. A. E. M. 1994 *Dynamics and modelling of ocean waves*. Cambridge Univeristy Press, Cambridge, UK

Lorenc, A. C. 1981 A global three-dimensional multivariate statistical interpolation scheme. *Mon. Weather Rev.*, **109,** 701–721

1986 Analysis methods for numerical weather prediction. *Q. J. R. Meteorol. Soc.*, **112,** 1177–1194

Lorenc, A. C. and Hammon, O. 1988 Objective quality control of observations using Bayesian methods. Theory, and a practical implementation. *Q. J. R. Meteorol. Soc.*, **114,** 515–543

Lönnberg, P. 1989 'Developments in the ECMWF analysis system'. Pp. 75–120 in Vol I of proceedings of ECMWF seminar on 'Data assimilation and the use of satellite data', 5–9 September 1988, ECMWF, Reading, UK

Lott, F. and Miller, M. 1997 A new sub-grid scale orographic drag parametrization: its formulation and testing. *Q. J. R. Meteorol. Soc.*, **123,** 101–127

McMillin, L. M. and Dean, C. 1982 Evaluation of a new operational technique for producing clear radiances. *J. Appl. Meteorol.*, **21,** 1005–1014

McNally, A. P. and Vesperini, M. 1996 Variational analysis of humidity information from TOVS radiances. *Q. J. R. Meteorol. Soc.*, **122,** 1521-1544

Parrish, D. F. and Derber, J. C. 1992 The National Meteorological Center's spectral statistical interpolation analysis system. *Mon. Weather Rev.*, **120,** 1747–1763

Phalippou, L. 1996 Variational retrieval of humidity profile, wind speed and cloud liquid-water path with the SSM/I: Potential for numerical weather prediction. *Q. J. R. Meteorol. Soc.*, **122,** 327–355

Phalippou, L. and Gérard, É. 1996 'Use of precise microwave imagery in numerical weather forecasting'. Study report to the European Space Agency. (Available from ECMWF, Reading, UK)

Phillips, N. A. 1986 The spatial statistics of random geostrophic modes and first-guess errors. *Tellus*, **38A,** 314–332

Rabier, F., Klinker, E., Courtier, P. and Hollingsworth, A. 1996a Sensitivity of forecast errors to initial conditions. *Q. J. R. Meteorol. Soc.*, **122,** 121–150

Rabier F., Thépaut, J.-N. and Courtier, P. 1996b 'Four dimensional variational assimilation at ECMWF'. In proceedings of ECMWF seminar on 'Data assimilation', 2–6 September 1996, ECMWF, Reading, UK

Rabier, F., McNally, A., Andersson, E., Courtier, P., Undén, P., Eyre, J., Hollingsworth, A. and Bouttier, F. 1998 The ECMWF implementation of three-dimensional variational assimilation (3D-Var). II: Structure functions. *Q. J. R. Meteorol. Soc.*, **124,** 1809–1829

Reale, A. L., Gray, D. G., Chalfont, M. W., Swaroop, A. and Nappi, A. 1986 'Higher resolution operational satellite retrievals'. Pp. 16–19 in preprints of the 2nd conference on 'Satellite meteorology/remote sensing and applications', Williamsburg, 13–16 May 1986, American Meteorological Society, Boston, USA

Ritchie, H., Temperton, C., Simmons, A., Hortal, M., Davies, T., Dent, D. and Hamrud, M. 1995 Implementation of the semi-lagrangian method in a high-resolution version of the ECMWF forecast model. *Mon. Weather Rev.*, **123,** 489–514

Savijärvi, H. 1995 Error growth in a large numerical forecast system. *Mon. Weather Rev.*, **123,** 212–221

Shaw, D. B., Lönnberg, P., Hollingsworth, A. and Undén, P. 1987 Data assimilation: The 1984/85 revision of the ECMWF mass and wind analysis. *Q. J. R. Meteorol. Soc.*, **114,** 533–566

Stoffelen, A. and Anderson, D. 1997 Ambiguity removal and assimilation of scatterometer data. *Q. J. R. Meteorol. Soc.*, **123,** 491–518

Talagrand, O. and Courtier, P. 1987 Variational assimilation of meteorological observations with the adjoint vorticity equation. I: Theory. *Q. J. R. Meteorol. Soc.*, **113,** 1311–1328

Thépaut, J.-N., Courtier, P., Belaud, G. and Lemaître, G. 1996 Dynamical structure functions in a four-dimensional variational assimilation: A case study. *Q. J. R. Meteorol. Soc.*, **122,** 535–561

Tiedtke, M. 1993 Representation of clouds in large-scale models. *Mon. Weather Rev.* **121,** 3040–3061

Tomassini, M., LeMeur, D. and Saunders, R. 1998 Satellite wind observations of hurricanes and their impact on NWP model analyses and forecasts. *Mon. Weather Rev.*, **126,** 1274–1286

Undén, P. 1989 Tropical data assimilation and analysis of divergence. *Mon. Weather Rev.* **117,** 2495–2517